

A Monte Carlo method for nuclear evaporation and fission at intermediate energies

A.Deppman^a, O.A.P.Tavares^b, S.B.Duarte^b, J.D.T. Arruda-Neto^{a,c}, M. Gonçalves^{e,f}, V.P. Likhachev^a, J. Mesa^a, E.C. de Oliveira^b, S.R. de Pina^a, and O. Rodriguez^{a,d}.

^aInstituto de Física da Universidade de São Paulo
P.O.Box 66318 - CEP 05315-970
São Paulo, Brazil

^bCentro Brasileiro de Pesquisas Físicas -CBPF/MCT
22290-180 Rio de Janeiro, Brazil

^cUniversidade de Santo Amaro - UNISA
São Paulo, Brazil

^dInstituto Superior de Ciencias y Tecnología Nucleares - ISCTN
A.P. 6163 La Habana, Cuba

^eInstituto de Radioproteção e Dosimetria - IRD/CNEN
22780-160 Rio de Janeiro, Brazil

^fSociedade Educacional São Paulo Apóstolo- UniverCidade
22710-260 Rio de Janeiro, Brazil.

April 3, 2003

Abstract

We describe a Monte Carlo method to calculate the characteristics of the competition between particle evaporation and nuclear fission processes taking place in the compound nucleus formed after the intranuclear cascade following the absorption of intermediate energy photons by the nucleus. In this version we include not only neutrons, but also protons and alphas as possible evaporating particles. However, this method allows an ease inclusion of other evaporating particles, as deuteron or heavier clusters. Some results for ^{237}Np , ^{238}U , and ^{232}Th are shown.

pacs: 25.85.Jg, 25.20.-x, 25.85.-w

I. INTRODUCTION

Nuclear reactions with intermediate or high energy photons are well described as a two-step process. In the first step, the incident photon interacts with one nucleon or a cluster of nucleons inside the nucleus, and then the energy transferred to these particles are redistributed to other nucleons by an intranuclear cascade process. During this step of the nuclear reaction, some particles may escape from the nucleus, thus reducing the total energy of the compound system. In the second step, the nuclear evaporation, the excitation energy is distributed among all the remaining nucleons, i.e., the residual nucleus reaches a thermodynamical equilibrium. At this step the nucleus may undergo fission, and it is the competition between particle evaporation and fission processes that determines the particle multiplicities and the fissility of the photonuclear reaction.

Until the beginning of the nineties it was believed that the fissility (W) of actinide nuclei should saturate at 100% for energies above $\sim 100\text{MeV}$ [1–4], leading several groups to propose research projects devoted to the systematic investigation of the photoabsorption process at intermediate and high energies by measuring the photofission cross section. In fact, since $W = 1$, photofission cross section measurements would allow an easy and direct evaluation for the total nuclear photoabsorption cross section [4–6] for heavy nuclei.

However, it was found with the experimental results for the photofissility of ^{232}Th that W is $\sim 60\%$ to $\sim 80\%$ of that for ^{238}U in the energy interval $200 - 1200\text{MeV}$ [4]. In this regard, a phenomenological description of the photofissility[10] suggested that the non-saturation of photofissility in ^{232}Th could be a consequence of its higher nuclear transparency, comparatively to that of ^{238}U , and a model based on nuclear structure was proposed in Ref. [11] to explain these findings. Photofission results for ^{237}Np reported by the Novosibirsk group[3] revealed a photofissility for ^{237}Np nearly 30% higher than that for ^{238}U in the energy interval $60 - 240\text{MeV}$. These results were confirmed quite recently by Sanabria and collaborators[12]. Finally, in a recent experiment performed at the Photon Tagging Facility in Hall B at the Thomas Jefferson Laboratory, Cetina et al.[13] thoroughly demonstrated that the photofission cross section for ^{238}U is about 80% of that for ^{237}Np up to $\sim 4\text{GeV}$. These findings have several implications on nuclear structure aspects[1, 4, 11], on the compound nucleus formation mechanisms[10], and on the potentialities of the fission channel as a probe to infer new nuclear reactions characteristics[4, 5].

In order to understand the experimental photofission results, it is necessary an ability to correctly calculate the characteristics of the intranuclear cascade as well as the evaporation-fission competition. In this paper we develop a method to calculate the second step of the photonuclear reaction, which allow us to obtain the nuclear photofission and evaporating-particles multiplicity.

II. THEORETICAL BACKGROUND

The probability for the emission of a particle j with kinetic energy between E_k and $E_k + dE_k$ is calculated according to the Weisskopf's statistical model[18] as,

$$P_j(E_k) dE_k = \gamma_j \sigma_j E_k \left(\frac{\rho_f}{\rho_i} \right) dE_k, \quad (1)$$

where σ_j is the nuclear capture cross section of particle j by the final nucleus, $\gamma_j = gm/(\pi^2 h^3)$, g denotes the number of spin states, and m is the particle mass. The level density for the initial and final nuclei, ρ_i and ρ_f , respectively, are calculated by the Fermi gas expression

$$\rho(E_j^*) = \exp\left(2(aE_j^*)^{\frac{1}{2}}\right), \quad (2)$$

where a is the level density parameter, and

$$E_j^* = E^* - (B_j + V_j). \quad (3)$$

E^* is the nuclear excitation energy in the initial state, B_j is the particle separation energy, and V_j is the Coulomb potential barrier corrected for the nuclear temperature, τ , defined as $\tau = [E^*/a]^{1/2}$.

The particle emission width is calculated as

$$\Gamma_j = \int_0^{E_j^*} P_j(E_k) dE_k. \quad (4)$$

From this general equation, we obtain the k -particle emission probability relatively to j -particle emission, that is

$$\frac{\Gamma_k}{\Gamma_j} = \left(\frac{\gamma_k}{\gamma_j} \right) \left(\frac{E_k^*}{E_j^*} \right) \left(\frac{a_j}{a_k} \right) \exp \left\{ 2 \left[(a_k E_k^*)^{\frac{1}{2}} - (a_j E_j^*)^{\frac{1}{2}} \right] \right\}. \quad (5)$$

The level density parameter for neutron emission is[19]

$$a_n = 0.134A - 1.21 \cdot 10^{-4} A^2 MeV^{-1}, \quad (6)$$

and for all other particle emission this quantity is related to a_n by

$$a_j = r_j a_n, \quad (7)$$

where r_j is a dimensionless constant.

The shell model corrections[20] are not taken into account, since they are small at intermediate excitation energies and are likely to cancel with each other on the average over all possible nuclei created during the reaction.

Using the fission width from the liquid drop model for fission by Bohr and Wheeler[21], and the neutron emission width from Weisskopf[18], we get[22]

$$\frac{\Gamma_f}{\Gamma_n} = K_f \exp \left\{ 2 \left[\left(a_f E_f^* \right)^{\frac{1}{2}} - \left(a_n E_n^* \right)^{\frac{1}{2}} \right] \right\}, \quad (8)$$

where

$$K_f = K_0 a_n \frac{\left[2 \left(a_f E_f^* \right)^{\frac{1}{2}} - 1 \right]}{\left(4A^{\frac{2}{3}} a_f E_n^* \right)}, \quad (9)$$

and

$$E_f^* = E^* - B_f, \quad (10)$$

with $K_0 = 14.39 MeV$. B_f is the fission barrier height discussed below.

For proton emission we get

$$\frac{\Gamma_p}{\Gamma_n} = \left(\frac{E_p^*}{E_n^*} \right) \exp \left\{ 2 \left(a_n \right)^{\frac{1}{2}} \left[\left(r_p E_p^* \right)^{\frac{1}{2}} - \left(E_n^* \right)^{\frac{1}{2}} \right] \right\}, \quad (11)$$

and for alpha particle emission

$$\frac{\Gamma_\alpha}{\Gamma_n} = \left(\frac{2E_\alpha^*}{E_n^*} \right) \exp \left\{ 2 \left(a_n \right)^{\frac{1}{2}} \left[\left(r_\alpha E_\alpha^* \right)^{\frac{1}{2}} - \left(E_n^* \right)^{\frac{1}{2}} \right] \right\}. \quad (12)$$

The Coulomb potential[23] (see Eq. (3)) for proton is

$$V_p = C \frac{[K_p (Z - 1) e^2]}{\left[r_0 (A - 1)^{\frac{1}{3}} + R_p \right]}, \quad (13)$$

and for alpha particle

$$V_\alpha = C \frac{[2K_\alpha (Z - 2) e^2]}{\left[r_0 (A - 4)^{\frac{1}{3}} + R_\alpha \right]}, \quad (14)$$

where $K_p = 0.70$ and $K_\alpha = 0.83$ are the Coulomb barrier penetrabilities for protons and alpha particles, respectively, $R_p = 1.14fm$ is the proton radius, $R_\alpha = 2.16fm$ is the alpha-particle radius, $r_0 = 1.2fm$, and

$$C = 1 - \frac{E^*}{B} \quad (15)$$

is the charged-particle Coulomb barrier correction due to the nuclear temperature [23], with B as the nuclear binding energy. In addition, we use $r_p = r_\alpha = 1$, as prescribed in Ref. [24].

The fission barrier is calculated by[20]

$$B_f = C(0.22(A - Z) - 1.40Z + 101.5)MeV; \quad (16)$$

the neutron binding energy is given by[20]

$$B_n = (-0.16(A - Z) + 0.25Z + 5.6)MeV, \quad (17)$$

while the proton and alpha-particle binding energies are respectively calculated by the expressions

$$B_p = m_p + m(A - 1, Z - 1) - m(A, Z), \quad (18)$$

and

$$B_\alpha = m_\alpha + m(A - 4, Z - 2) - m(A, Z), \quad (19)$$

where m_p is the proton mass, m_α is the alpha particle mass, and $m(A, Z)$ is the nuclear mass calculated with the parameters from Ref. [25].

The present Monte Carlo method for Evaporation-Fission (MCEF) calculates, at the i^{th} step of the evaporation process, the nuclear fission probability defined as

$$F_i = \frac{\left(\frac{\Gamma_f}{\Gamma_n}\right)_i}{1 + \left(\frac{\Gamma_f}{\Gamma_n}\right)_i + \left(\frac{\Gamma_p}{\Gamma_n}\right)_i + \left(\frac{\Gamma_\alpha}{\Gamma_n}\right)_i}, \quad (20)$$

with the quantities Γ_f/Γ_n , Γ_p/Γ_n and Γ_α/Γ_n calculated as in equations (8), (11) and (12), respectively. Then, the evaporating particle (neutron, proton or alpha) is chosen randomly, according to their relative branching ratios (see equation (5)). Once one of these particles is chosen, the mass and atomic numbers are recalculated as

$$A_{i+1} = A_i - \Delta A_i, \quad (21)$$

and

$$Z_{i+1} = Z_i - \Delta Z_i, \quad (22)$$

where ΔA_i , and ΔZ_i , are, respectively, the mass and atomic numbers of the ejected particle at the i^{th} step in the evaporation process. Also, the nuclear excitation energy is modified according to the expression

$$E_{i+1}^* = E_i^* - B_i - T_i, \quad (23)$$

where B_i and T_i are the separation and the asymptotic kinetic energies of the ejected particle, respectively. For neutrons, $T = 2MeV$, for protons $T = V_p$, and for alpha particles $T = V_\alpha$.

Expression (23) ensures that the nuclear excitation energy is smaller, at each step in the evaporation chain, than it was in the previous step. This process continues until the excitation energy available in the nucleus is not enough to emit any of the possible evaporating particles. At this point the evaporation process stops, and we can calculate the nuclear fissility by the expression

$$W = \sum_i \left[\prod_{j=0}^{i-1} (1 - F_j) \right] F_i. \quad (24)$$

III. THE MONTE CARLO METHOD

The statistical character of the intermediate energy photonuclear reaction leads us to use the Monte Carlo method for a more detailed and precise study of this process. In nuclear evaporation and fission competition, the nuclear reaction may develop itself in many different ways for the same initial conditions, preventing the use of deterministic methods.

The evaporation step initiates when the intranuclear cascade finishes. The main parameters are the atomic and mass numbers and the excitation energy of the residual nucleus formed at the end for the cascade. Our Monte Carlo method to calculate the nuclear evaporation and fission processes is performed by the following steps, also schematically described in figure 1:

- 1) From the nuclear mass and atomic numbers, and using the nuclear excitation energy, it calculates the fission barrier, as in eq. (16), the separation energies for neutron, proton, and alpha-particle, by using eqs. (17), (18) and (19), respectively, and the respective Coulomb barriers given in eqs. (13) and (14).
- 2) It verifies if the excitation energy is high enough to allow the emission of any particle or fissioning. If possible, the particle emission probability is calculated for each of the possible evaporating particles using expressions $P_j = (\Gamma_j/\Gamma_n) / [1 + (\Gamma_p/\Gamma_n) + (\Gamma_\alpha/\Gamma_n)]$,

with j corresponding to neutrons (n), prótons (p) and alpha-particles (α) . If no process is allowed at this excitation energy, step 7 is performed.

- 3) A random number r is generated, and the emitting particle is chosen using this number and the probabilities calculated in step 2. First, r is compared with the proton emission probability. If $r < P_p$, a proton escapes from the nucleus. If not $P_p < r < P_p + P_\alpha$, then an alpha-particle is emitted. If none of these possibilities is verified, a neutron is emitted.
- 4) The probability the nucleus undergoes fission in this step is calculated by using expression (20).
- 5) The nuclear mass and atomic numbers are recalculated considering the emission of the particle chosen in step 3, as shown in eqs. (21) and (22).
- 6) The excitation energy of the new residual nucleus is calculated according to the particle emitted, by using equation (23). Then, we go back to step 1.
- 7) The nuclear fissility is calculated using formula (24), and the evaporation process halts.

As this process is essentially statistical, as shown in step 3, for the same input parameters we can have different results when running the algorithm a second time. To take into account this feature of the entire process, we need to run several times the above procedure. The final results are then understood as mean values of the desired physical parameter investigated, as the fissility or particle multiplicity. The software implementation of this model can be found in reference [26].

IV. RESULTS

By using the model described above we have calculated the fissility for ^{232}Th relative to ^{238}U , and that for ^{238}U and ^{232}Th relative to ^{237}Np . Although the multicollisional code in its present version is more accurate for energies above 500MeV , we noticed that the relevant distributions of A_c , Z_c and E_c for the compound nuclei are approximately independent of the incident photon energies in the intermediate energy range[14]. Therefore, we extended our model down to 200MeV as the lower limit of our calculation.

In Figure 2 we show our results for the relative fissility for ^{232}Th and ^{238}U with respect to ^{237}Np , and experimental data for comparison. As in the previous case, we observe that our results provide a good description for the slowly varying behavior of the relative fissility for ^{238}U and ^{232}Th from 200MeV to 1000MeV , the approximate saturation being thus reproduced. Also, absolute values are in good agreement with the data for both nuclei, with values ranging from ~ 0.45 to ~ 0.60 for ^{232}Th , and from ~ 0.75 to ~ 0.90 for ^{238}U .

These results show that our nuclear-evaporation/fission model, associated with the multi-collisional Monte Carlo for the intranuclear cascade process, gives a good description for the photofissility data. Also, this model allows us to verify the important role played by proton and alpha particle emissions during the evaporation stage, as processes leading to the non-saturation of the photofissility. We performed the fissility calculations allowing only neutron evaporation, and the results, presented in Figure 3, largely overestimate the experimental fissilities.

These and other results are analysed in more details in reference[27].

V. CONCLUSIONS

This paper describes the model we developed to calculate the properties of nuclear-evaporation and fission decay channels after intermediate-energy photon absorption by actinide nuclei.

We have shown that this model allowed to find a solution for a long-standing problem of actinides, namely, that their fissility saturates at values smaller than 100%, even at relatively high energies. The key modeling ingredients are the description of the intranuclear cascade with the MCMC algorithm, and the inclusion of proton and alpha-particle as possible evaporating particles.

We acknowledge the support from the Brazilian agencies FAPESP and CNPq.

-
- [1] J. Ahrens et al., Phys. Lett. B146, 303 (1984).
 - [2] A. Lepretre et al., Nucl. Phys. A472, 533 (1987).
 - [3] A. S. Iljinov et al., Nucl. Phys. A539, 263 (1992).

- [4] N. Bianchi et al., Phys. Rev. C48, 1785 (1993).
- [5] N. Bianchi et al., Phys. Lett. B299, 219 (1993).
- [6] Th. Frommhold et al., Phys. Lett. B295, 28 (1992).
- [7] J. Ahrens, Nucl. Phys. A446, 229c (1985).
- [8] J. D. T. Arruda-Neto et al., Phys. Lett. B248, 34 (1990).
- [9] G. J. Miller et al., Nucl Phys A551, 135 (1993).
- [10] J. D. T. Arruda-Neto et al., Phys. Rev. C51, 751 (1995).
- [11] A. Deppman et al.; Nuovo Cimento 109A, 1197 (1996).
- [12] J. C. Sanabria et al.; Phys. Rev. C61, 034604 (2000).
- [13] C. Cetina et al., Phys. Rev. Lett. 84, 5740 (2000).
- [14] M. Gonçalves et al.; Phys. Lett B406, 1 (1997).
- [15] V. Muccifora et al., Phys. Rev. C60, 064616 (1999).
- [16] H. W. Bertini; Phys. Rev. 131, 1801 (1963).
- [17] V. S. Barashenkov et al.; Nucl. Phys. A231, 462 (1974).
- [18] V. F. Weisskopf, Phys. Rev. 52, 295 (1937).
- [19] A. S. Iljinov, E. A. Cherepanov, and S. E. Chigrinov, Yad. Fiz. 32, 322 (1980) [Sov. J. Nucl. Phys. 32, 166 (1980)].
- [20] C. Guaraldo et al., Nuovo Cimento. 103A, 607 (1990).
- [21] N. Bohr and J. A. Wheeler, Phys. Rev. 56, 426 (1939).
- [22] R. Vandenbosch and J. R. Huizenga, Nuclear Fission, (1sted., New York Academic Press, 1973) p227.
- [23] O. A. P. Tavares and M. L. Terranova, Z. Phys. A: Hadr. and Nucl. 343, 407 (1992).
- [24] K. J. LeCouteur, Proc. Phys. Soc. Lond., Ser. A63, 259 (1950).
- [25] E. Segrè, Nuclei and Particles, (3rded., W. A. Benjamin, INC, 1965) p215.
- [26] A. Deppman et al., accepted for publication in Comp. Phys. Comm. (2002).
- [27] A. Deppman et al., Phys. Rev. Lett 87 (2001) 182701.

VI. FIGURE CAPTIONS

Figure 1: Schematic view of the seven steps in the evaporation/fission model described in this paper.

Figure 2: Relative fissility for ^{232}Th and ^{238}U with respect to that for ^{237}Np . Full lines are the results of our calculations and dotted lines indicate the statistical uncertainties due to the Monte Carlo calculation. The experimental data are taken from Ref. [13].

Figure 3: Relative fissility for ^{232}Th (dashed line) and ^{238}U (dot-dashed line) with respect to that for ^{237}Np , now considering that only neutrons can evaporate from the nucleus, in competition with the fission process. The experimental data are the same as in Fig. 2.

Figure 1

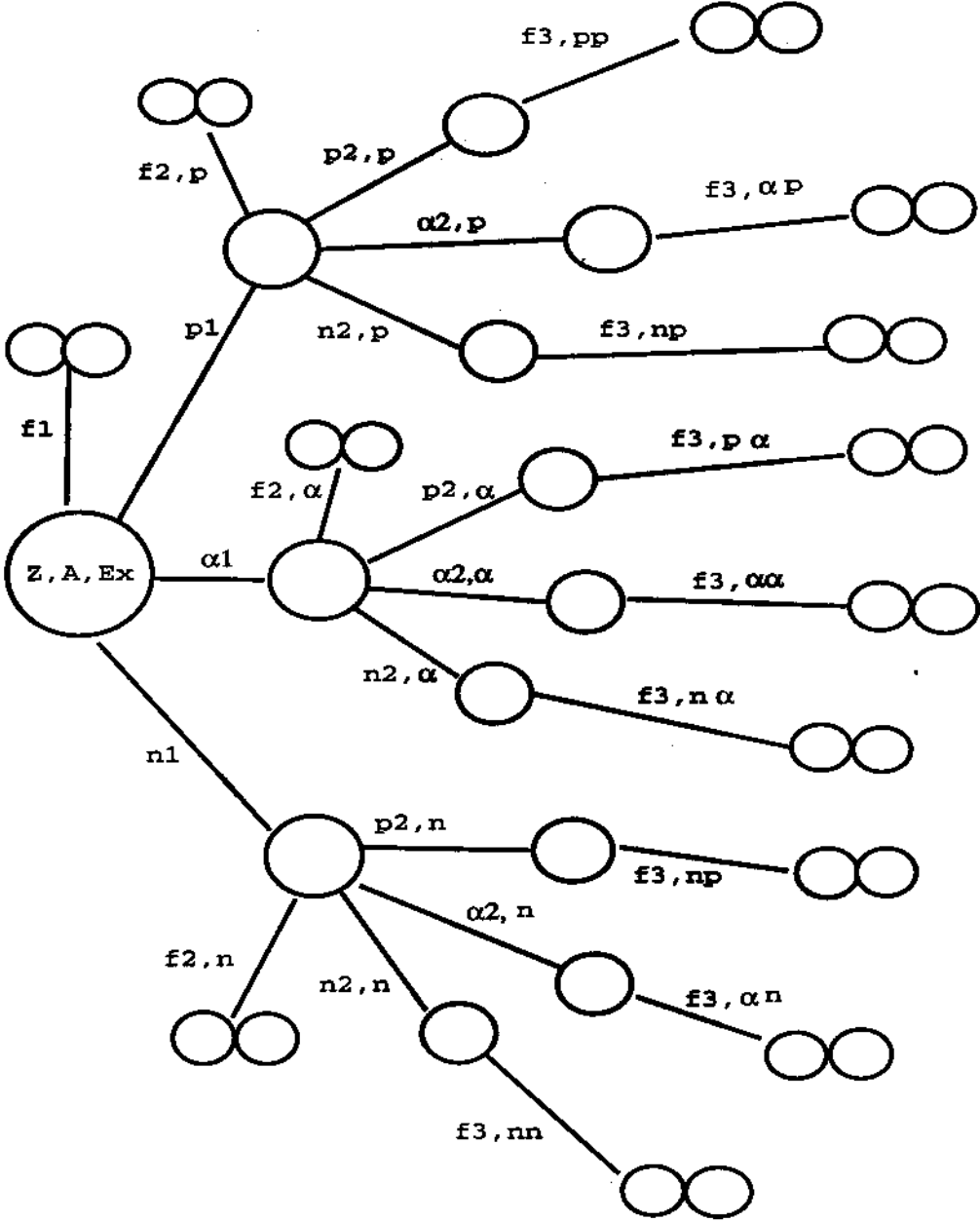


Figure 2

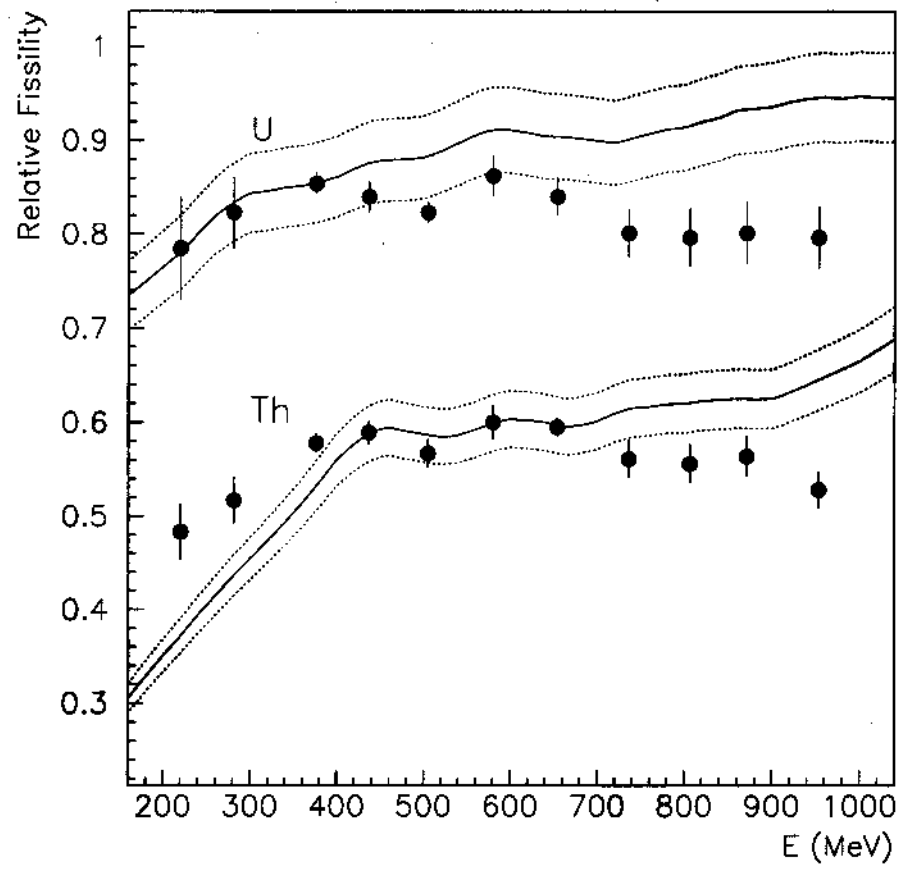


Figure 3

